SAND2008-3101 C

SAND2008-3101C

Inducing and Imaging Localized Passivity Breakdown in Aluminum using an AFM Approach

K. R. Zavadil

Sandia National Laboratories, Albuquerque NM, 87185-0888, USA

The impact of localized polarization of aluminum in aqueous chloride is studied using *in situ* atomic force microscopy (AFM). The primary goal of this study is to determine whether nanostructural degradation in the form of passivity loss and pit initiation can be induced by applying potential pulses between a conductive AFM probe tip and an aluminum surface. Nanoscopic imaging of the mechanically compliant hydrous oxide on an Al(111) textured film with 0.5 wt.% Cu is demonstrated. A correlation is made between characteristic nanostructural changes observed for localized and macroscopic area polarization. Pit initiation proximity to the AFM tip is also demonstrated arguing for millisecond time periods as being sufficient to drive pit initiation within a targeted area. A significant degree of spatial variance in proximity is observed, which suggests a larger length scale, intrinsic susceptibility to pit initiation not dictated by known structural heterogeneity like grain boundary structure.

Introduction

The process of localized corrosion resulting in pitting in a variety of passive metals is preceded by a series of electrochemically observable and unobservable events. Metastable pits often form that are readily observable on macro-length scale electrodes owing to the fact that a period of pit growth occurs producing current transients with lifetimes on the order of seconds (1). Moving earlier in time and smaller in event size, pit nucleation events can be monitored provided sufficiently smaller electrodes, fast acquisition times, and ultra-low current sensitivity electrometers are all used. Direct imaging of these events is a difficult challenge because no *a priori* knowledge exists as to where such an event might take place. Yet, it is reasonable to assume that localized changes in composition and/or structure of the passive oxide take place representing passive oxide breakdown prior to the onset of the local discharge of the underlying metal that signals one of these pre-pitting events. These localized changes have not been directly observed to occur at a site that then undergoes pit nucleation. Establishing a causal link between oxide breakdown and pitting would provide valuable information on the initiation mechanism of pits.

Several strategies exist that appear to be reasonable approaches to knowing where to expect a breakdown event: 1) building in a weak link in a model passive metal system so as to accurately anticipate the location of a breakdown site, 2) restricting the electrode size to such a dimension that the imaging method used fully samples all regions of the electrode, and 3) inducing oxide breakdown in a predetermined location by locally polarizing a specific site on the surface. The latter approach has the advantage of being applicable to any material system of interest without the requirement of adding

sensitizing defects, applying masking techniques, or fabricating micro-electrodes. An electrode can be locally polarized by using relatively fast potential pulses with a counter electrode that is placed closed to the working electrode under investigation. This technique has been used to conduct localized dissolution of metals in aqueous electrolytes at sub-micron spatial resolution (2,3). The same approach can be used to conduct local deposition (4,5). Localization of the interfacial potential drop at the working electrode:electrolyte interface required for the reduction/oxidation reaction is produced by matching the time the potential is applied to the time required for development of the local potential. This time is given by the product of the interfacial capacitance and the resistance of the electrolyte path between the counter and working electrodes. This time value is approximately 10^1 ns for specific capacitance values of 10 $\mu F \cdot cm^{-2}$, electrolyte resistivities of 10 $\Omega \cdot cm$, and tip-surface separations of 1 μm.

An atomic force microscope platform is well adapted for this concept of combining local polarization with imaging. In AFM imaging, precise distances are maintained and measured between the imaging tip and imaged surface. All that is required is a conductive tip and a method for controlling the potential difference between the tip and surface for a desired time period. Typical native oxides on aluminum exhibit interfacial capacitance values of 15 $\mu F \cdot cm^{-2}$ in 200 $\Omega \cdot cm$ NaCl, arguing that pulse widths of 300 ns should be sufficiently short to localize interfacial potential for a 1 μm separation. No previous attempts at conducting this combined experiment on an oxide passivated metal have been reported in the literature. This report describes initial attempts at conducting this combined experiment. The work is focused on overcoming challenges related to imaging a mechanically compliant interface, correlating anticipated surface nanostructure from conventional corrosion experiments with that created under conditions of localized polarization, and demonstrating the pit initiation can be induced in proximity to the imaging tip.

Experimental

Aluminum thin films were sputter deposited onto a titanium nitride:titanium overlayer on Si(100) using an Applied Materials Endura deposition system. Target film thicknesses were 700 nm using a deposition rate of 20 $nm \cdot s^{-1}$ and a substrate temperature of 175ºC. The deposition target was a solid solution of 0.5 wt.% copper in aluminum. A native oxide was allowed to form after substrate cooling to room temperature by exposure to the laboratory ambient. The native oxide thickness was confirmed to be 3.1 nm using time-of-flight secondary ion mass spectrometry (TOF-SIMS) in a sputter depth profiling mode. Sputter rate calibration for TOF-SIMS was achieved using an oxide on a pure aluminum thin film whose thickness was measured by transmission electron microscopy for a cross-sectioned sample.

Polarization experiments were conducted on an Agilent 5500 AFM instrument. Nanosensors EFM probes with a Pt/Ir coating were used as the counter electrode and imaging device. A target tip-film distance of 400 nm was used during the potential pulse. These chips were ozone cleaned for approximately one hour, mounted on the manufacturer's chip holder, and the chip body was hand painted with a toluene diluted polydimethylsiloxane (RTV 3411, Dow Corning). This electrical insulation of the underside of the chip resulted in the tip and the underside of the cantilever as the two metalized surfaces most closely spaced with respect to the aluminum substrate. Imaging

was conducted using amplitude modulation at relatively low free amplitude values (2 nm) and at as high an amplitude set point as possible. These conditions led to an ability to image in an attractive mode, a necessary condition for imaging the highly mechanically compliant hydrous outer layer of the passive oxide on aluminum. Electrolytes were formed from high purity HCl (Fluka UltraTrace) and 18 MΩ·cm water (Barnstead NANOpure Infinity system). Solution pH was adjusted with low carbonate NaOH (Fluka UltraTrace). Solution resistivity for a 50 mM NaCl electrolyte was measured to be 210 Ω·cm. All electrochemical measurements were conducted in a N_2 de-aerated electrolyte. Post-polarization site imaging was conducted on a Zeiss Supra 55VP field emission scanning electron microscope.

Results & Discussion

In situ Imaging of a Mechanically Complaint Hydrous Oxide

The surface topography of the passive oxide on the [111] facets is characterized by an oxide platelet structure. An example of this structure is shown in Figure 1a for the as-deposited Al film. This secondary electron micrograph shows a large [111] facet at the

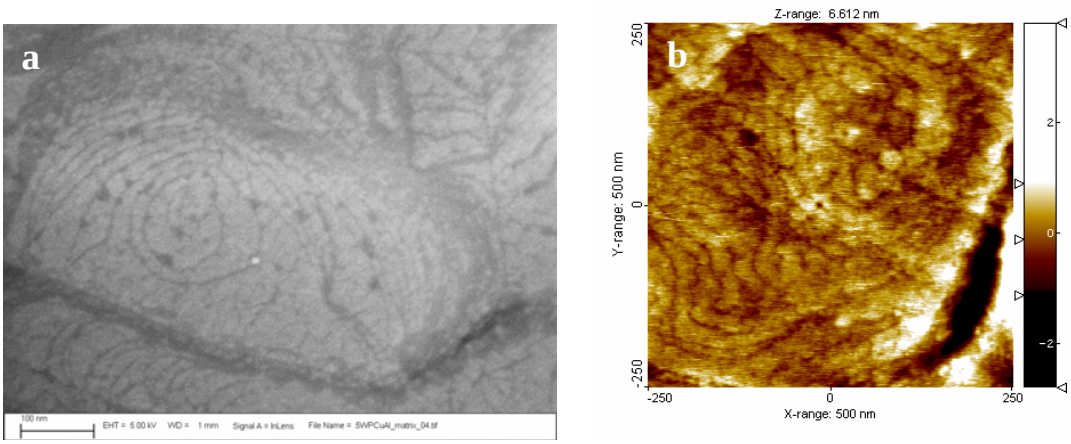

Figure 1. a) FE-SEM images of an as-deposited Al:0.5 wt% Cu film highlighting the oxide platelet morphology on an Al(111) facet and b) attractive AM-AFM image of this same film in 50 mM NaCl exhibiting the same platelet structure.

approximate image center bounded by a grain boundary at angles in the lower portion of the image. These facets possess the remnants of terrace-step structure from the original vapor phase deposition of the aluminum film, as evidenced by the presence of contour lines whose spacing decrease along the regions of incline on the grain. Oxidation of these surfaces to form the native 3 nm thick oxide require significant place exchange between surface oxygen and sub-surface aluminum. For a 3.0 $g \cdot cm^{-3}$ oxide, oxide formation must also accommodate an approximate 1.7 relative specific volume increase. This combination of oxide nucleating at step edges, lateral material movement, and compressive stress leads to platelet formation where these platelets follow the contours of the original growth steps. The platelets are not continuous along the growth steps and exhibit discontinuities that appear as circular recesses along their perimeter boundaries. The platelets are also segmented with bisecting boundaries that run at various angles with respect to the step edges. A good deal of this detail appears to be maintained when the film is immersed in an aqueous electrolyte, as shown in Fig. 1b. A [111] facet is shown

bounded by a grain boundary at the lower right quadrant of this *in situ* AFM image. Platelets arranged along contours with circular discontinuities and bisecting boundaries are displayed in this image. The similarity between these images demonstrates that high fidelity images of nanoscopic detail are possible using attractive mode, *in situ* imaging of the passive oxide on aluminum even though the outer surface is a mechanically compliant hydrous oxide. This level of detail is the basis for using AFM as a method of correlating morphological changes with induced, localized electrochemical processes.

The response of a film surface to a slow rate, anodic potentiodynamic scan provides an idea of what type of morphological changes are expected under conditions just prior to stable pitting. Scanning the potential of the film from its equilibrium potential (open circuit) to more positive values (anodic polarization) has the effect of increasing the net rate of aluminum oxidation, as well as making the oxide:electrolyte interface more electropositive. The consequence of these two interfacial changes is that the oxide may grow in thickness, nanoscale structure such as voids and subsequent pores may form and grow from ionic vacancy reactions, and Cl^- will accumulate within the outer region of the oxide (6). Slow rate polarization allows sufficient time for the induction of passivity breakdown, which is related to Cl^- accumulation and possibly related to nanostructure evolution, as exhibited by observable pit nucleation and metastable pitting events. Figure 2a shows a potentiodynamic scan conducted in de-aerated 50 mM NaCl at a scan rate of 167 $\mu V \cdot s^{-1}$. The film exhibits a low passive current density of 50 $nA \cdot cm^{-2}$ shortly after

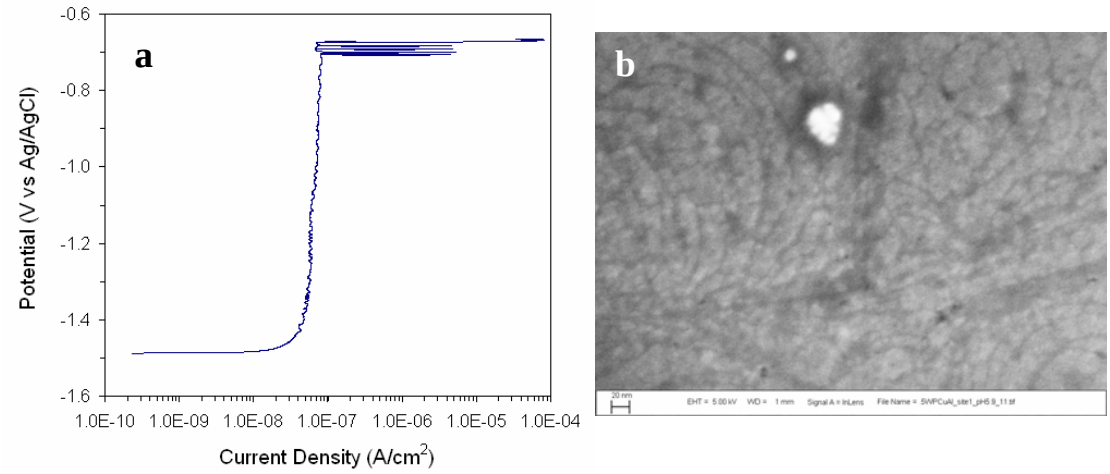

Figure 2. a) Potentiodynamic response of an as-deposited Al:0.5 wt% Cu film in 50 mM NaCl at a scan rate of 167 $\mu V \cdot s^{-1}$ b) FE-SEM image of the film polarized to stable pit formation in de-aerated 50 mM NaCl at a scan rate of 167 $\mu V \cdot s^{-1}$.

polarizing from open circuit. Low values of current density of 80 $nA \cdot cm^{-2}$ are maintained up to a potential of -700 mV. Four individual metastable pit transients with peak currents of 4 to 5 $\mu A \cdot cm^{-2}$ are visible between -700 and -680 mV. At -673 mV, a pit initiates, grows, and becomes sufficiently stable to support a current density of 60 $\mu A \cdot cm^{-2}$. This event signals the onset of stable pitting.

Ex situ imaging was performed on this film after slow anodic polarization to correlate morphological changes with the polarization process. A representative SEM image is shown in Figure 2b. Two significant changes in surface morphology become evident when comparisons are made between this image and images generated from the as-

deposited film. The first of these changes is a shift from a platelet to a more nodular shape for the oxide. This change can be seen in the upper left quadrant of Fig. 2b where the contour lines are still visible for this [111] facet, but are defined by less elongated plates and more circular nodules. These nodules may result from potential induced restructuring of the hydrous oxide accompanied by Cl^- accumulation or by initial stages of potential-induced growth of additional oxide. The second change that takes place is the appearance of nanopores (or voids) within the oxide. These nanostructures show up as dark spots (regions of reduced secondary electron emission) at various locations in the lower fraction of Fig. 2. We propose that these nanostructures are created by an ionic vacancy pairing reaction (6). These morphological changes are subtle, in part, because the passive oxide regulates the overall extent of aluminum oxidation and extent of material conversion. An example of limited material conversion can be found in estimating the overall extent of oxide growth from the data of Fig. 2a. Integration of the charge density generated during this polarization scan yields a value of 0.35 $mC \cdot cm^{-2}$. In contrast, the oxidation of a single layer of aluminum atoms on a [111] facet would generate a charge density of 0.68 $mC \cdot cm^{-2}$. Conversion of a single Al(111) monolayer to an oxide with a density of 3.0 $g \cdot cm^{-3}$ would produce a 0.4 nm thickness increase in the passive oxide. The integrated charge density from Fig. 2a indicates that stable pitting can initiate with minimal material conversion or a fractional monolayer of oxide growth.

Imaging the Impact of Localized Polarization

Initial attempts at localized polarization were conducted using relatively long pulse widths in the millisecond time regime as opposed to a more optimized value of 300 ns. The primary purpose for using longer pulses was to ensure sufficient charge was generated during polarization to induce morphological changes that could be imaged and related to changes created by slow rate polarization. Large amplitude potential pulses of 1 V were used so as to exceed the stable pitting potential observed in potentiodynamic measurements (see Fig. 2a). The influence of applying a progressively longer pulse of 1 V from 0 to 5 ms is shown in Figure 3. The [111] oriented grain that appears in the approximate center of the 0 ms labeled image serves as a point of comparison. This grain exhibits a high growth step density along its left and lower perimeters with well defined oxide platelets arrayed along the contours. The top of the grain possesses the characteristic concentric rings of platelets with a number of approximately circular discontinuities expected for a [111] oriented facet. These basic structural features on the facet and along the grain perimeter remain unaltered for the first few pulses up through 3 ms. After a 4 ms pulse, the well defined platelets appear to have been disrupted with the formation of discrete nodules along the grain perimeter. The circular discontinuities on the facet are, however, still visible after the 4 ms pulse. After the 5 ms pulse, these discontinuity features are significantly obscured and the more pronounced nodular morphology has formed along the left and lower grain perimeters. We conclude that regions of high step density undergo the most significant change in local topology. These findings are consistent with higher rate, controlled current density polarization results where void and pore nucleation are shown to preferentially form along high gradient regions of [111] textured aluminum surfaces (7). These imaging results also highlight the fact that subtle changes can be monitored *in situ* and as a function of localized polarization of the aluminum film surface.

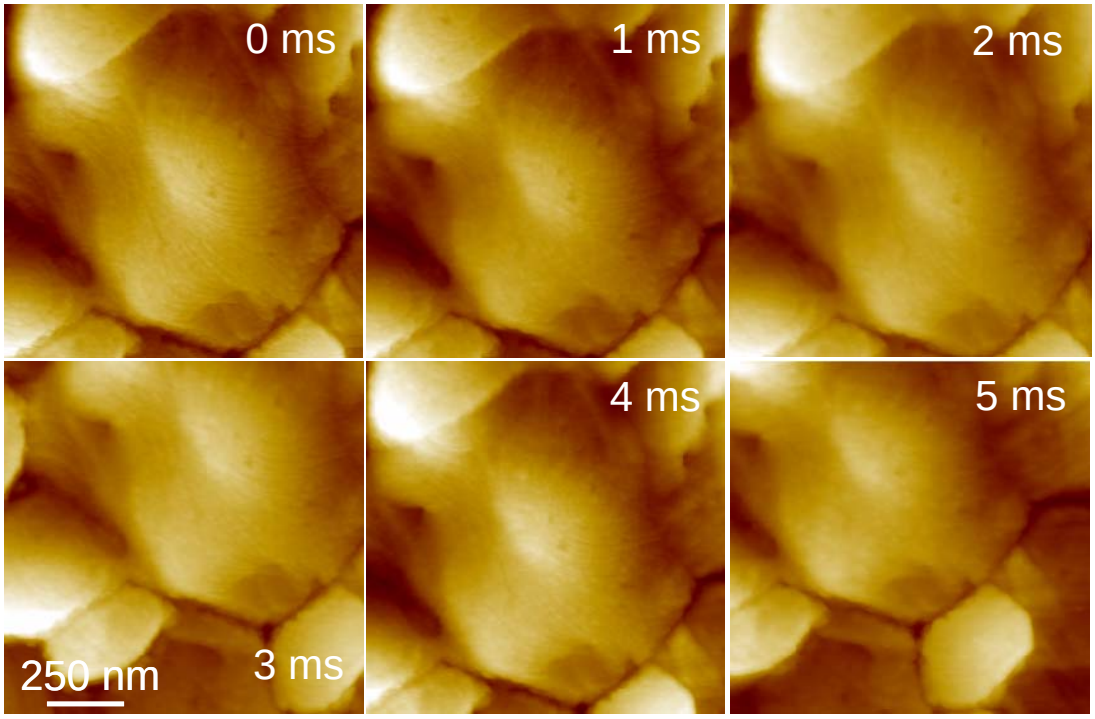

Figure 3. *In situ* AM-AFM monitoring of morphological changes on Al:0.5 wt% Cu in 50 mM NaCl induced by a series of 1 V pulses applied in sequence for progressively longer periods of time from 0 to 5 ms. The tip was raised 400 nm above the surface during potential application and then re-engaged to acquire the corresponding image, producing some degree of drift in the [111] facet of interest.

Longer time pulses produce additional anticipated changes in the local morphology as well as other discernable regional events. Figure 4 shows the impact of applying a 1 V pulse for a period of 1 second. The *in situ* AFM image shown in Fig. 4a demonstrates that pores have formed preferentially along facet perimeters and grain boundaries. The protruding [111] facet in the lower, right quadrant of this image exhibits a perimeter that is decorated with numerous pores. Pores are an anticipated nanostructural feature within this system based on the slow sweep potentiodynamic results discussed earlier in this paper. This preference for nanostructure nucleation and growth at high gradient sites appears quite similar to a pure Al(111) film's response to non-localized polarization as seen in the SEM image of Figure 4b. In this image a protruding [111] facet is shown to be surrounded by similarly sized pores. The fact that pores appear at a time interval longer than 5 ms may indicate limiting kinetics for the ion vacancy pairing reaction argued to give rise to these features.

One consequence to applying potential for longer periods of time is the loss of localized polarization. Figure 4c shows an optical micrograph that was created immediately after the pulse used to generate the data of Fig. 4a. A pit is shown in the upper right quadrant of the image. The formation of this pit during the pulse was observed in real time. The distance between the pit and the tip is on the order of several hundred microns. This results demonstrates that sufficient interfacial potentials are developed in time periods of 1 s and pit initiation is no longer constrained to take place in proximity of the probe tip.

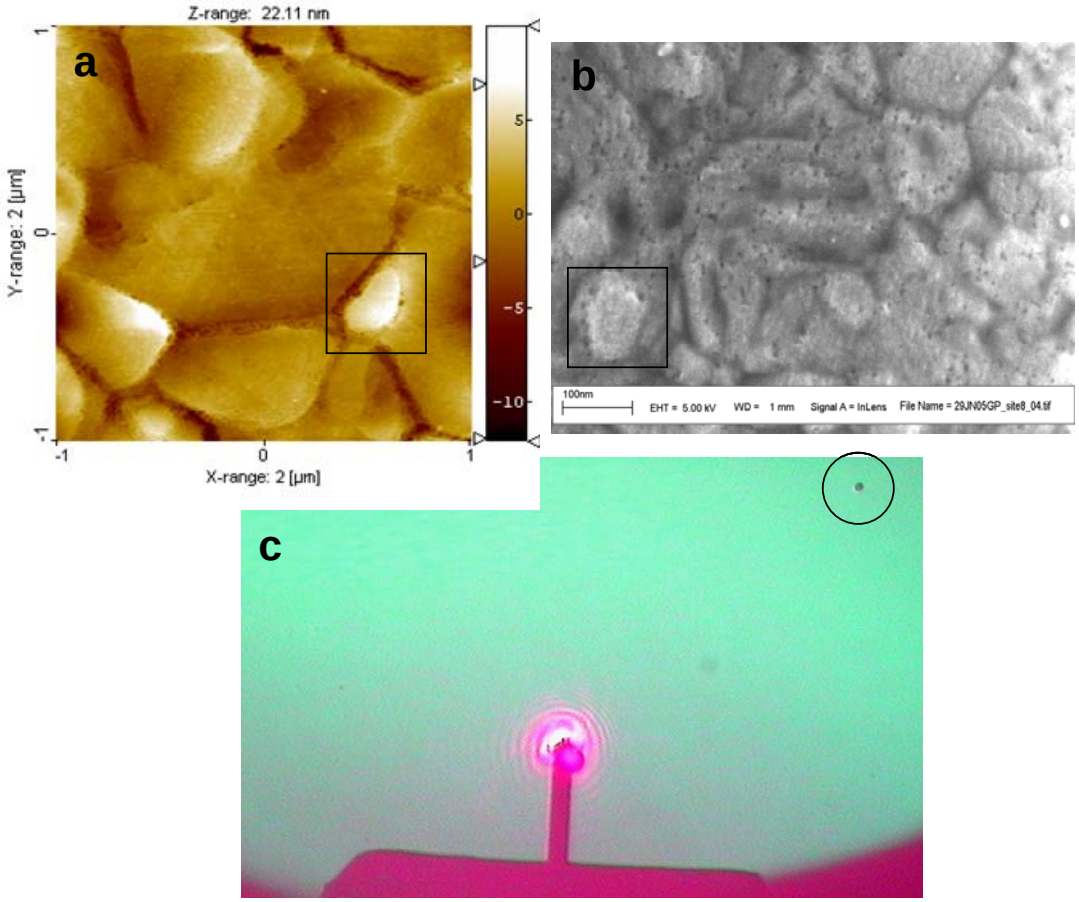

Figure 4. a) *in situ* AM-AFM image of an Al:0.5 wt% Cu film surface after the application of a 1 V potential pulse for 1 second in 50 mM NaCl – highlighted square designates [111] facet of interest, b) non-localized polarization of a pure Al film in 50 mM NaCl showing pore formation around a [111] facet (highlighted square), and c) optical image of a pit (highlighted circle) formed on the sample in panel **a** during 1 V, 1 s polarization.

Pit Initiation in Proximity of the Probe Tip

Pitting can be driven in the proximity to the tip provided short time pulses are used to localize polarization. Figure 5 shows the results of applying a 0 V, 1 ms pulse to the Al:0.5 wt% Cu film surface in 50 mM NaCl. The initial morphology for the target region of the surface is shown in Fig. 5a. Image quality is not particularly good in this instance and the doubling of facet and grain edge features appears to be the results of adherence of a particle to the AFM probe tip. The highlighted feature shown in the lower, center of Fig. 5a appears to be the result of an excessive repulsive interaction between the tip and sample. Just prior to acquiring this image, the cantilever amplitude was observed to undergo a large degree of damping during a controlled 400 nm withdrawal from the sample surface. Excessive damping suggests that the tip-surface distance may have actually been decreased resulting in a period of hard tapping of the surface with the tip. A second tip-surface separation of 400 nm followed by a 0 V potential pulse for 1 ms produced a pit adjacent to the highlighted defect of Fig. 5a. This pit is shown in Figure 5b.

A large fraction of grains A – D have been consumed by the final pit that measures approximately 1 μm in diameter. Of note is the fact that the original site of contact between the tip and sample is still present on the surface which suggests that the hard tapping may not have been responsible for initiating pitting. The original site can be seen in the insert to Figure 5b. The center of the pit is located within 0.6 μm of the original apparent tip-surface contact site. The overall approximate correlation between tip location during polarization and the resulting pit location demonstrates the degree to which localization should be ultimately possible in this type of experiment.

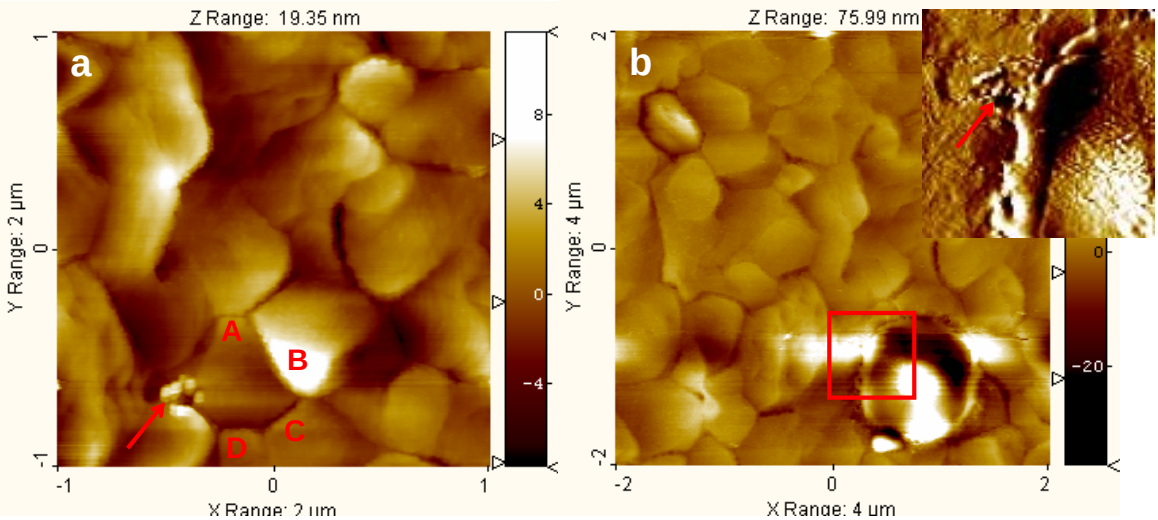

Figure 5. a) *in situ* AM-AFM image of an Al:0.5 wt% Cu film surface prior to localized polarization in 50 mM NaCl – arrow designates site of possible hard tapping by tip, and b) *in situ* image after applying a 0 mV, 1 ms pulse at a tip-film distance of 400 nm - highlighted square corresponds to the region of letter designated grains in panel **a**. The inset of panel **b** shows an amplitude mode image of the site of hard tapping after the pulse, where the arrow designates site location.

This ability to drive pitting in proximity to the tip has been reproduced a limited number of times using varying combinations of cell potential and pulse time. A limited degree of reproducibility validates this overall approach to inducing pit initiation based on local polarization. However, the fact that a degree of variation exists in both whether pitting occurs very near the probe tip and the conditions under which this proximal pitting occurs raises a number of questions and concerns. Observed variation in spatial proximity seems to argue that a significant variation in pit initiation probability exists across the surface of the film. In a nanocrystalline material where grain size is small, variation appears to rule out the typical explanations for pit initiation susceptibility such as grain boundary structure. The use of much shorter pulses to further localize the field will be required to better probe the origins of spatial variance. Estimates of the limits of localization based on electrochemical machining studies argue that 300 ns pulses will be required for localization of interfacial charging to sub-micron areas. A second concern involves the possibility that longer time periods than the pulse widths necessary for localization are required to induce pit nucleation and initiation at some average site on the surface. This potential difficulty might be overcome by imposing the potential pulse after first slowly sweeping the potential of the aluminum surface. Additional solutions to this problem include conducting repetitive pulses at some multiple of pulse period. An ability

to create an overall aluminum:passive oxide:electrolyte interface that simulates the electronic (potential distribution included) and chemical properties under near-steady state polarization will depend on how rapidly defects within this structure are extinguished with time.

Conclusions

A coupled electrochemical stimulus – response mapping technique has been demonstrated for the study of pit nucleation and initiation in the passive oxide on aluminum in aqueous chloride electrolytes. High fidelity *in situ* imaging of the mechanically compliant hydrous oxide surface on an aluminum thin film is demonstrated. An attractive mode amplitude modulation technique exhibits sufficient stability to image a variety of nanoscopic features on the Al(111) facets both prior to and after localized polarization. A correlation is established between various structural changes created by near steady state, non-local and pulsed, local polarization. These changes include the transition from oxide platelets on the surface to oxide nodules as well as the formation nanopores. The former change is argued to be driven by preferential growth of oxide at remnant step edges and the latter by an ion vacancy pairing reaction. Finally, pit initiation is shown to occur in proximity to the probe tip using millisecond pulse widths arguing for some degree of control over dictating the likely location of a pitting event. Significant spatial variance is observed in pit initiation location indicating an intrinsic susceptibility to pit initiation may exist within this material system.

Acknowledgments

The author wishes to thank J. Stevens for the Al film deposition and B. McKenzie for the SEM analysis. The support of the DOE/Basic Energy Sciences Office of Materials & Engineering Sciences is gratefully recognized. This work was supported by the United States Department of Energy under Contract DE-AC04-94AL85000. Sandia is a multiprogram laboratory operated by Sandia Corporation, a Lockheed Martin Company, for the United States Department of Energy's National Nuclear Security Administration.

References

1. Z. Szklarska-Smialowska, "Pitting & Crevice Corrosion," NACE International, Houston, TX, 2005.
2. R. Schuster, V. Kirchner, P. Allomgue and G. Ertl, *Science* **289**, 98 (2000).
3. M. Koch, V. Kirchner, R. Schuster, *Electrochim. Acta* **48**, 3213 (2003).
4. D.M. Kolb and F.C. Simeone, *Electrochim. Acta* **50**, 2989 (2005).
5. A.L. Trimmer, J.J. Maurer. R. Schuster, G. Zangari, and J.L. Hudson, *Chem Mater.* **17**, 6755 (2005).
6. K.R. Zavadil, J.A. Ohlhausen, and P.G. Kotula, *J. Electrochem. Soc.* **153**(8), B296 (2006).
7. K.R. Zavadil, P.G. Kotula, and J.A. Ohlhausen, ECS Trans. 1(4), 139 (2006).